Numerical studies of a granular gas in a host medium

M. Bisi †, S. Rjasanow ‡, G. Spiga †

† Dipartimento di Matematica, Università di Parma,
Viale G.P. Usberti 53/A, I-43100 Parma, Italy
marzia.bisi@unipr.it, giampiero.spiga@unipr.it
‡ Fachrichtung 6.1 - Mathematik, Universität des Saarlandes,
Postfach 151150, D-66041 Saarbrücken, Germany
rjasanow@num.uni-sb.de

Abstract

The nonlinear dissipative Boltzmann equation for a granular gas diffusing in a elastically scattering host medium is investigated and numerically solved by means of direct stochastic simulation. The procedure requires an appropriate treatment of the two collision integrals involved, and of their different features. The algorithm is first tested versus exact results for macroscopic moments worked out in the Maxwellian-pseudo-molecules approximation, and then it is applied to the more realistic collision model of hard spheres for both elastic and inelastic encounters. When collisions with background are dominant, reliability of some hydrodynamic closures is then discussed by comparison of their outputs to the kinetic results achieved by the present DSMC approach.

AMS Subject Classification: 82C40, 82C80, 65R20
Keywords: Granular matter, Boltzmann equation, Stochastic numerics

1 Introduction

Dilute granular flows have been widely investigated in recent years from many points of view, including experimental, numerical, and theoretical, and kinetic theory has naturally provided one of the most appropriate tools of investigation. We may quote, for example, without pretending to be exhaustive, [26, 23, 3, 15, 12, 4, 21, 10, 17]. Main feature of binary collisions between grains is that they are inelastic, since only a fraction of the normal relative impact velocity is restituted, so that these collisions dissipate kinetic energy, which is transferred to non–participating degrees of freedom, leading to a progressive loss of thermal energy of the grains themselves. There is thus no standard smooth equilibrium like the Maxwellian distribution of classical kinetic theory of rarefied gases [19, 18], but some equilibrium can be restored in the system in the presence of a supply of external energy, so that energy loss due to inelasticity may be balanced by an energy gain experienced by the grains. Indeed, there exists an extensive literature on granular gases driven

by different kinds of thermal bath: examples are provided, just to quote few of them, by [2, 13, 14, 27, 24]. It is remarkable that some of the most significant applications of granular gases concern diffusion of grains, fine powders, or small impurities in the atmosphere or in a given environment, and these processes may be modelled at the kinetic level in terms of binary encounters of tiny particles (the grains) against the field particles (scatterers) of a given background, constituting the host medium in which they are embedded. Models and methods from linear kinetic theory can then be properly applied [20], and in this frame the test particles of the granular gas exchange momentum and energy with the background, which (being much denser by definition) is instead essentially unaffected by the interactions going on. In this way, grains can actually gain energy by collision (supposed elastic for simplicity) from the host medium, and such a gain could balance the energy loss due to inelastic collisions of the grains between themselves. To this research line belong for instance [5, 30, 32, 25, 8, 9, 7]. Results concern particular solutions and exact equilibria for the so–called Pseudo–Maxwellian model introduced by [12], while, for the more realistic collision model of hard spheres, iterative numerical schemes or Sonine polynomial expansions for the relevant kinetic equations have been developed, as well as the investigation of the proper hydrodynamic regime corresponding to the asymptotic limit when evolution is dominated by collisions of grains with the background particles. Possible dependence of the restitution coefficient on impact speed and impact angle can also be taken into account. The only hydrodynamic variable in this frame is granular mass, but suitable closure strategies have been devised in order to include also mass velocity and granular temperature in the hydrodynamic description.

The present paper aims at proceeding further along the last research line above. We shall consider specifically the Boltzmann type equation for the distribution function of a granular gas embedded in a scattering background, whose collision term is made up by two collision integrals. The first one is linear and elastic, and accounts for interaction of grains with the background, modelled, as usual, for simplicity, as binary encounters with some field particles (see [9] for details). The second one is nonlinear and inelastic, and describes collision of grains between themselves, with dissipation of kinetic energy. The linear operator conserves mass of both test and field particles, plus overall momentum and energy of the two species. It would drive the test particle distribution function towards a local equilibrium at the background velocity and temperature. The nonlinear operator conserves mass and momentum of the granular gas, and would drive granular temperature to zero. The question on whether these competing effects can balance has been answered by [25], where existence of a collision equilibrium has been proved for realistic collision models. We shall tackle the above kinetic equation (in its space homogeneous form, in this first approach) by direct numerical stochastic simulation [6, 28]. DSMC methods are widely used in kinetic theory, both elastic and inelastic [22, 29], but their application to combined dissipation and background effects at collision level is new, to our knowledge, and quite challenging. For reasons of numerical efficiency, the time evolution of the system is often approximated via a splitting technique using some time step $\Delta t > 0$. This leads to a decoupling of physical effects. However, an additional numerical error will be the price, see [29] for more details. In the present paper, we develop an algorithm without the DSMC-error due to splitting technique and illustrate that the error depends on two discretization parameters: on the number of particles n and on the number N_{rep}

of independent ensembles generated.

Results can be used in particular to test other collision models, and to check macroscopic trends predicted by fluid–dynamic equations in the relevant asymptotic limit. An useful comparison tool is provided by the Maxwell–molecule collision kernel [11], in which case the exact moment equations in space homogeneous conditions are closed, and then one can compute mass velocity, temperature and all macroscopic fields of interest by simply solving a system of nonlinear ODEs. For more realistic collision models, these kinetic results are not subject to any restriction on the pertinent Knudsen number, but provide a crucial benchmark for the hydrodynamic closures obtained when such a parameter tends to zero, like those proposed in [9].

The paper is organized as follows. In Section 2, we give a short description of the inelastic Boltzmann equation embedded in a scattering background. We present here both exact solutions for the evolution of macroscopic parameters obtained from the Maxwellian model, and hydrodynamic closures obtained for the more realistic model of hard spheres when collision with the background is the dominant process. In Section 3, we describe the main components of the stochastic solution of the above kinetic Boltzmann equation and formulate two stochastic numerical algorithms for this equation. In Section 4, we present the results of our numerical tests. Here we use the analytically known time relaxation of the bulk velocity and of the temperature for the model of Maxwell pseudo-molecules for a careful check of the convergence. The numerical results obtained for the hard sphere collision model are then compared with the hydrodynamic descriptions.

2 Boltzmann equation for an inelastic gas in a host medium

Let us consider the space homogeneous kinetic equation

$$\frac{\partial f}{\partial t} = J_{EL}(f, f^B) + J_{IN}(f, f)\,, \tag{1}$$

where J_{EL} is the linear elastic operator describing collisions with the host medium (labelled by a superscript B), and J_{IN} is the inelastic operator describing collisions between grains themselves, as described in the Introduction. Resorting to the unit vector $\hat{\omega}$ along the post–collision relative velocity, the elastic scattering operator has the standard form

$$J_{EL}(f, f^B) = \int\limits_{\mathbb{R}^3} \int\limits_{S^2} B_1(|\mathbf{g}|, \hat{\omega}) \Big[f(\mathbf{v}')\, f^B(\mathbf{w}') - f(\mathbf{v}) f^B(\mathbf{w}) \Big] d\mathbf{w}\, d\hat{\omega}\,,$$

where $\mathbf{g} = \mathbf{v} - \mathbf{w}$ is the pre–collision relative velocity, while f^B denotes the fixed and steady background Maxwellian distribution

$$f^B = \rho^B\, M^B = \rho^B \left(\frac{m^B}{2\pi T^B} \right)^{3/2} \exp\left(- \frac{m^B}{2T^B} \left| \mathbf{v} - \mathbf{u}^B \right|^2 \right)$$

at assigned number density ρ^B, mass velocity $\mathbf{u}^B$, and temperature T^B. Post–collision velocities are given by

$$\begin{aligned} \mathbf{v}' &= (1-\alpha)\mathbf{v} + \alpha\,\mathbf{w} + \alpha|\mathbf{g}|\,\hat{\omega}\,, \\ \mathbf{w}' &= (1-\alpha)\mathbf{v} + \alpha\,\mathbf{w} - (1-\alpha)|\mathbf{g}|\,\hat{\omega}\,, \end{aligned} \tag{2}$$

where α is the mass ratio

$$\alpha = \frac{m^B}{m+m^B}\,. \tag{3}$$

The inelastic collision integral, characterized by a restitution coefficient $e \in (0,1)$ along the apse line, reads as

$$J_{IN}(f,f) = \int\limits_{\mathbb{R}^3}\int\limits_{S^2} B_2(|\mathbf{g}|,\hat{\omega})\Big[\chi\, f(\mathbf{v}_*)\, f(\mathbf{w}_*) - f(\mathbf{v})f(\mathbf{w})\Big]d\mathbf{w}\, d\hat{\omega}\,,$$

where now $\mathbf{v}_*$ and $\mathbf{w}_*$ are the pre–collision velocities corresponding to $\mathbf{v}$ and $\mathbf{w}$ (different from the post–collision ones, $\mathbf{v}^*$ and $\mathbf{w}^*$) and χ is the Jacobian of the transformation ($\chi = 1/e^2$ if e is independent from collision parameters). Post–collision velocities are the most significant, since they enter explicitly both the numerical simulations and the weak forms of the kinetic Boltzmann equation (1), and are given by

$$\begin{aligned} \mathbf{v}^* &= \frac{1+\beta}{2}\,\mathbf{v} + \frac{1-\beta}{2}\,\mathbf{w} + \frac{1-\beta}{2}\,|\mathbf{g}|\,\hat{\omega}\,, \\ \mathbf{w}^* &= \frac{1-\beta}{2}\,\mathbf{v} + \frac{1+\beta}{2}\,\mathbf{w} - \frac{1-\beta}{2}\,|\mathbf{g}|\,\hat{\omega}\,, \end{aligned} \tag{4}$$

where

$$\beta = \frac{1-e}{2}\,, \tag{5}$$

with $0 < \beta < 1/2$. The weak forms of the two collision operators are indeed

$$\begin{aligned} \int\limits_{\mathbb{R}^3} \varphi(\mathbf{v})\, J_{EL}(f,f)\, d\mathbf{v} &= \int\limits_{\mathbb{R}^3}\int\limits_{\mathbb{R}^3}\int\limits_{S^2} B_1(|\mathbf{g}|,\hat{\omega})\Big[\varphi(\mathbf{v}') - \varphi(\mathbf{v})\Big] f(\mathbf{v}) f^B(\mathbf{w})\, d\mathbf{v}\, d\mathbf{w}\, d\hat{\omega}\,, \\ \int\limits_{\mathbb{R}^3} \varphi(\mathbf{v})\, J_{IN}(f,f^B)\, d\mathbf{v} &= \int\limits_{\mathbb{R}^3}\int\limits_{\mathbb{R}^3}\int\limits_{S^2} B_2(|\mathbf{g}|,\hat{\omega})\Big[\varphi(\mathbf{v}^*) - \varphi(\mathbf{v})\Big] f(\mathbf{v}) f(\mathbf{w})\, d\mathbf{v}\, d\mathbf{w}\, d\hat{\omega} \end{aligned} \tag{6}$$

and it is immediately seen that Eq. (1) preserves mass (number of grains) so that the number density

$$\rho = \int_{\mathbb{R}^3} f(\mathbf{v})\, d\mathbf{v} \tag{7}$$

remains constant in our problem. The same is not true for mass velocity and temperature of the granular gas, defined as

$$\mathbf{u} = \frac{1}{\rho}\int\limits_{\mathbb{R}^3} \mathbf{v}\, f(\mathbf{v})\, d\mathbf{v}\,, \qquad\qquad T = \frac{1}{3}\,\frac{m}{\rho}\int\limits_{\mathbb{R}^3} |\mathbf{v}-\mathbf{u}|^2\, f(\mathbf{v})\, d\mathbf{v}\,, \tag{8}$$

since J_{EL} prescribes exchange of momentum and energy with the background, while J_{IN} guarantees conservation of granular momentum, but enforces loss of energy due to inelasticity ($e < 1$, or $\beta > 0$). Exact macroscopic evolution equations (not closed, in general) for $\mathbf{u}$ and T are essentially obtained as weak forms of Eq. (1) corresponding to the test functions $\varphi(\mathbf{v}) = \mathbf{v}$ and $\varphi(\mathbf{v}) = |\mathbf{v}|^2$. A rather common expression for the restitution coefficient is given by the law [33]

$$1 - e = 2\,\beta_0\,\gamma(|\mathbf{g}\cdot\hat{\mathbf{n}}|) \qquad \text{where} \qquad \gamma(r) = r^\delta\,, \tag{9}$$

with $\beta = \beta_0\,\gamma$ representing the degree of inelasticity. The option $\delta = 0$ reproduces the case of constant restitution coefficient, while $\delta = 1/5$ corresponds to the so–called viscoelastic spheres [16]. Here $\hat{\mathbf{n}}$ denotes the unit vector in the direction of the apse line, which bisects the angle between $\mathbf{v} - \mathbf{w}$ and $-\hat{\omega}$; more precisely

$$|\mathbf{g}\cdot\hat{\mathbf{n}}|^2 = \frac{1}{2}\Big[|\mathbf{g}|^2 - |\mathbf{g}|(\mathbf{g}\cdot\hat{\omega})\Big]\,. \tag{10}$$

For constant restitution coefficient, and in the frame of the so–called Pseudo–Maxwellian model [12], it was shown in [32] that Eq. (1) admits a unique equilibrium distribution, which turns out to be a Maxwellian at the background velocity $\mathbf{u}^B$ and at a temperature $T^* < T^B$ which can be explicitly computed in terms of mass ratio and inelasticity coefficients α and β. This result was extended to the more realistic case of collision kernels B_1 and B_2 representing hard spheres interactions in [25]. The existence of equilibrium solutions to the inelastic Boltzmann equation in a background has been also proved when even scattering with the host particles is inelastic, and the background distribution is different from the classical Maxwellian shape [7]. The problem of a fluid–dynamic closure of the macroscopic equations for ρ, $\mathbf{u}$, T following from the space dependent version of Eq. (1) was addressed in [9] for a general restitution coefficient of the form (9) and for hard sphere collisions, in terms of entropy maximization under moment constraints, by resorting to either the relative entropy (local equilibrium approximation) or the quadratic entropy (Grad–type expansion), both quite popular in linear kinetic theory. The underlying assumption was of course an asymptotic regime in which elastic scattering with the host medium plays the dominant role in the process.

We shall resume such closures in space homogeneous conditions as a comparison test for the stochastic numerical approach described later. We focus now our attention on the case of constant restitution coefficient ($\delta = 0$ in (9)) and of collision kernels relevant to Maxwell–molecule interactions, both for grain–background and for grain–grain encounters. In other words, we shall take [28]

$$B_1(|\mathbf{g}|,\hat{\omega}) = C_1\,, \quad B_2(|\mathbf{g}|,\hat{\omega}) = C_2 \tag{11}$$

with C_1 and C_2 positive constants. This Maxwell–type assumption allows in fact to express all power moments of the collision integrals J_{EL} and J_{IN} in terms of the corresponding (unknown) moments of the distribution function, and to achieve thus a closed set of exact ordinary differential equations for the sought fields $\mathbf{u}$ and T. Here ρ is a constant and we may scale distribution functions as $f = \rho\,\tilde{f}$ and $f^B = \rho^B\,\tilde{f}^B$ (so that $\tilde{\rho} = \tilde{\rho}^B = 1$ in the numerical approach). Also we may use a dimensionless time $\tilde{t} = \rho^B\,C_1\,t$, which amounts

to using the mean test particle - field particle collision time as time unit. This leads to the appearance of the dimensionless parameter (Knudsen number)

$$Kn = \frac{\rho\, C_2}{\rho^B\, C_1} > 0\,, \tag{12}$$

ratio of the elastic to the inelastic mean collision time. If the dimensionless time variable is re–labelled as t, governing equations take, after some simple algebra, the form

$$\begin{aligned} \frac{d\mathbf{u}}{dt} &= -\,4\,\pi\,\alpha\,(\mathbf{u}-\mathbf{u}^B), \\ \frac{dT}{dt} &= \frac{8}{3}\,\pi\Big[m\,\alpha^2|\mathbf{u}-\mathbf{u}^B|^2 - 3\,\alpha(1-\alpha)(T-T^B)\Big] - \pi\,Kn\,(1-e^2)\,T, \end{aligned} \tag{13}$$

where Kn is not subject to any restriction. Mass velocity is easily found to be

$$\mathbf{u}(t) = \mathbf{u}^B + (\mathbf{u}_0 - \mathbf{u}^B)\exp\left(-\,4\,\pi\,\alpha\,t\right) \tag{14}$$

with exponential relaxation to its equilibrium value $\mathbf{u}^B$. Equation for T is a bit more involved, but standard manipulations yield the closed form solution

$$T(t) = T_0\,\mathrm{e}^{-\,Ct} + \frac{D}{C}\left(1-\mathrm{e}^{-\,Ct}\right) + \frac{A}{C-B}\left(\mathrm{e}^{-\,Bt} - \mathrm{e}^{-\,Ct}\right), \tag{15}$$

for $B \neq C$, or

$$T(t) = T_0\,\mathrm{e}^{-\,Bt} + \frac{D}{B}\left(1-\mathrm{e}^{-\,Bt}\right) + At\mathrm{e}^{-\,Bt} \tag{16}$$

for $B = C$, where

$$\begin{aligned} A &= \frac{8}{3}\,\pi\,m\,\alpha^2\,|\mathbf{u}_0-\mathbf{u}^B|^2\,, \\ B &= 8\,\pi\,\alpha\,, \\ C &= 8\,\pi\,\alpha(1-\alpha) + \pi\,Kn\,(1-e^2)\,, \\ D &= 8\,\pi\,\alpha\,(1-\alpha)\,T^B\,. \end{aligned} \tag{17}$$

Granular temperature relaxes then to its equilibrium value

$$T^* = \frac{D}{C} = \frac{8\,\alpha\,(1-\alpha)\,T^B}{8\,\alpha(1-\alpha) + Kn\,(1-e^2)} < T^B. \tag{18}$$

In the more realistic case of hard sphere collisions (both elastic and inelastic) and with a general δ in (9), the previous analytical procedure can not be pursued. We refer the interested reader to [9], where suitable hydrodynamic closures have been achieved in the hypothesis that the pertinent Knudsen number (ratio of the elastic to the inelastic mean free path) is small. Now collision kernels read as

$$B_1(|\mathbf{g}|,\hat{\omega}) = C_1\,|\mathbf{g}|\,, \qquad B_2(|\mathbf{g}|,\hat{\omega}) = C_2\,|\mathbf{g}|\,, \tag{19}$$

of course with a different meaning of constants C_i with respect to (11), since now they are related to the sphere diameters d and d^B by

$$C_1 = \frac{1}{4}\left(\frac{d+d^B}{2}\right)^2, \qquad C_2 = \frac{1}{4}\,d^2\,. \tag{20}$$

It proves convenient here resorting to the scaled time variable $\bar{t} = (\rho^B/\rho)\,\rho^B\,C_1\,t$ (whose dimension is an inverse speed). We shall restrict our numerical computations to hard–sphere collisions with constant restitution coefficient (i.e. $\delta = 0$ and $\beta = \beta_0 = (1-e)/2$). Then, rearranging the fluid–dynamic equations worked out in [9] and removing again all bars, closure by local equilibrium approximation yields

$$\begin{aligned}
\frac{\partial \mathbf{u}}{\partial t} &= -\,\alpha\,\frac{16}{3}\sqrt{2\pi}\sqrt{\frac{\alpha\,m}{(1-\alpha)T^B+\alpha\,T}}\left[\frac{1}{5}|\mathbf{u}-\mathbf{u}^B|^2+2\,\frac{(1-\alpha)T^B+\alpha\,T}{\alpha\,m}\right](\mathbf{u}-\mathbf{u}^B)\,,\\
\frac{\partial T}{\partial t} &= \alpha\,\frac{8}{3}\,m\,\sqrt{2\pi}\sqrt{\frac{\alpha\,m}{(1-\alpha)T^B+\alpha\,T}}\left\{\frac{1}{5}\left[\alpha+\frac{1}{3}\,\frac{\alpha\,T}{(1-\alpha)T^B+\alpha T}\right]|\mathbf{u}-\mathbf{u}^B|^4\right.\\
&+4\,\frac{(1-\alpha)T^B+\alpha\,T}{\alpha\,m}\left[\alpha-\frac{1}{3}\,\frac{\alpha\,T}{(1-\alpha)T^B+\alpha T}\right]|\mathbf{u}-\mathbf{u}^B|^2\\
&\left.+8\left[\frac{(1-\alpha)T^B+\alpha\,T}{\alpha\,m}\right]^2\left[\alpha-\frac{\alpha\,T}{(1-\alpha)T^B+\alpha T}\right]\right\}\\
&-\frac{64}{3}\,\sqrt{\pi}\,\mathcal{K}\,m\,\beta\,(1-\beta)\left(\frac{T}{m}\right)^{3/2},
\end{aligned} \tag{21}$$

while in the case of Grad–type approximation one ends up with

$$\begin{aligned}
\frac{\partial \mathbf{u}}{\partial t} &= -\,\sqrt{\alpha}\,\frac{32}{3}\,\sqrt{\pi}\sqrt{\frac{2T^B}{m}}(\mathbf{u}-\mathbf{u}^B)\,,\\
\frac{\partial T}{\partial t} &= -\,\sqrt{\alpha}\,\frac{64}{3}\,\sqrt{\pi}\sqrt{\frac{2T^B}{m}}\left\{(1-\alpha)(T-T^B)-\frac{1}{3}\,\alpha\,m|\mathbf{u}-\mathbf{u}^B|^2\right\}\\
&-\frac{4}{3}\,\sqrt{\pi}\,\mathcal{K}\,m\,\beta\,(1-\beta)\left\{\frac{1}{3}\left[\frac{m}{T^B}|\mathbf{u}-\mathbf{u}^B|^2+3\,\frac{T-T^B}{T^B}\right]^2+8\,\frac{(3\,T-T^B)}{T^B}\right\}\left(\frac{T^B}{m}\right)^{3/2}.
\end{aligned} \tag{22}$$

Now a dimensionless parameter

$$\mathcal{K} = \left(\frac{\rho}{\rho^B}\right)^2\frac{C_2}{C_1} = \frac{\rho}{\rho^B}\;Kn \tag{23}$$

shows up, which must be small in the physical scenario of [9] (in other words, ρ must be smaller than ρ^B).

Integration of the two different hydrodynamic models (21) and (22) yields results which are not distinguishable, as they should, for $\mathcal{K} < 10^{-1}$, whereas, for $\mathcal{K}$ increasing up to values of order unity, a small but clear discrepancy appears and enlarges in the temperatures (velocities remain overlapped, though). In the numerical computations presented later on, kinetic results will be compared to those of the simpler dynamical system (22), and differences with respect to (21) will be described and discussed when necessary.

3 Direct Stochastic Simulation

3.1 General description

The main idea of all particle methods for the Boltzmann type equations (see [28] and especially [34] for the linear elastic collisions with the background) is an approximation of the time dependent family of measures

$$f(t,\mathbf{v})\,d\mathbf{v}\,,\ t\in\mathbb{R}_+$$

by a family of point measures

$$\mu^{(n)}(t,d\mathbf{v})=\frac{1}{n}\sum_{j=1}^{n}\delta_{\mathbf{v}_j(t)}(d\mathbf{v})$$

defined by the system of particles

$$\Big(\mathbf{v}_1(t),\ldots,\mathbf{v}_n(t)\Big)\,. \tag{24}$$

Thus the weights of the particles are $1/n$ and $\mathbf{v}_j(t)\in\mathbb{R}^3$ denote their velocities. The measure $\mu^{(n)}$ approximates the solution f of the Boltzmann equation (1) in the sense that

$$\lim_{n\to\infty}\frac{1}{n}\sum_{j=1}^{n}\varphi(\mathbf{v}_j(t))=\int\limits_{\mathbb{R}^3}\varphi(\mathbf{v})\,f(t,\mathbf{v})\,d\mathbf{v}\,, \tag{25}$$

where φ is any appropriate test function. The behaviour of the system (24) can be described as follows. The first step is an approximation of the initial measure

$$f_0(\mathbf{v})\,d\mathbf{v}$$

by a system of particles (24) for $t=0$. Then the elastic and inelastic collisions take place in randomly distributed discrete time points. While the inelastic collisions dissipate the kinetic energy of the particles, the elastic collisions with the background prevent the system from becoming frozen. The "collision step" is the most crucial part of the whole procedure. The behaviour of the collision process is as follows: the waiting time τ between the collisions is a random variable with the distribution

$$\mathrm{Prob}\,\{\tau\geq t\}=\exp(-\hat{\pi}\,t)\,,$$

where

$$\hat{\pi}=\sum_{1\leq i\leq n}E_1(\mathbf{v}_i)+\frac{1}{2\,n}\sum_{1\leq i\neq j\leq n}E_2(\mathbf{v}_i,\mathbf{v}_j)=\hat{\pi}_1+\hat{\pi}_2\,,$$

where

$$E_1(\mathbf{v}_i) \;=\; \int\limits_{\mathbb{R}^3}\int\limits_{S^2}B_1(|\mathbf{v}_i-\mathbf{w}|,\hat{\omega})\,f^B(\mathbf{w})\,d\hat{\omega}\,d\mathbf{w}\,, \tag{26}$$

$$E_2(\mathbf{v}_i,\mathbf{v}_j) \;=\; \int\limits_{S^2}B_2(|\mathbf{v}_i-\mathbf{v}_j|,\hat{\omega})\,d\hat{\omega}\,. \tag{27}$$

With the probability

$$\frac{\hat{\pi}_1}{\hat{\pi}_1 + \hat{\pi}_2}$$

the elastic collision with the background takes place, and, with the probability

$$\frac{\hat{\pi}_2}{\hat{\pi}_1 + \hat{\pi}_2}\,,$$

the inelastic binary collision takes place. If an elastic collision with the background has to be realised then the following steps are to perform. Choose an index $i \in \{1, \ldots, n\}$ corresponding to the discrete probabilities

$$\frac{E_1(\mathbf{v}_i)}{\displaystyle\sum_{1 \le j \le n} E_1(\mathbf{v}_j)}\,, \quad i = 1, \ldots, n\,.$$

For given i, generate a velocity $\mathbf{w} \in \mathbb{R}^3$ corresponding to the probability density

$$\frac{\displaystyle\int_{S^2} B_1(|\mathbf{v}_i - \mathbf{w}|, \hat{\omega})\, d\hat{\omega}}{\displaystyle\int_{\mathbb{R}^3}\int_{S^2} B_1(|\mathbf{v}_i - \mathbf{z}|, \hat{\omega})\, f^B(\mathbf{z})\, d\hat{\omega}\, d\mathbf{z}}\, f^B(\mathbf{w})\,.$$

For given i and $\mathbf{w}$, generate $\hat{\omega} \in S^2$ corresponding to the probability density

$$\frac{B_1(|\mathbf{v}_i - \mathbf{w}|, \hat{\omega})}{\displaystyle\int_{S^2} B_1(|\mathbf{v}_i - \mathbf{w}|, \hat{\omega})\, d\hat{\omega}}\,.$$

Perform the collision transformation (2), i.e. replace the velocity $\mathbf{v}_i$ by

$$\mathbf{v}_i' = (1 - \alpha)\mathbf{v}_i + \alpha\mathbf{w} + \alpha|\mathbf{v}_i - \mathbf{w}|\,\hat{\omega}\,,$$

where α is the mass ratio (3). For an inelastic binary collision, first choose an index pair $i, j \in \{1, \ldots, n\}$ with $i \neq j$ corresponding to the discrete probabilities

$$\frac{E_2(\mathbf{v}_i, \mathbf{v}_j)}{\displaystyle\sum_{1 \le k \ne l \le n} E_2(\mathbf{v}_k, \mathbf{v}_l)}\,, \quad i, j = 1, \ldots, n\,.$$

For given i, j, generate $\hat{\omega} \in S^2$ corresponding to the probability density

$$\frac{B_2(|\mathbf{v}_i - \mathbf{v}_j|, \hat{\omega})}{\displaystyle\int_{S^2} B_2(|\mathbf{v}_i - \mathbf{v}_j|, \hat{\omega})\, d\hat{\omega}}\,.$$

Perform the collision transformation (4), i.e. replace the velocities $\mathbf{v}_i\,, \mathbf{v}_j$ by

$$\mathbf{v}_i^* = \frac{1+\beta}{2}\,\mathbf{v}_i + \frac{1-\beta}{2}\,\mathbf{v}_j + \frac{1-\beta}{2}\,|\mathbf{v}_i - \mathbf{v}_j|\,\hat{\omega}\,,$$
$$\mathbf{v}_j^* = \frac{1-\beta}{2}\,\mathbf{v}_i + \frac{1+\beta}{2}\,\mathbf{v}_j - \frac{1-\beta}{2}\,|\mathbf{v}_i - \mathbf{v}_j|\,\hat{\omega}\,,$$

where β is the inelasticity parameter (5). This procedure has to be repeated until the final time of the simulation is reached. Thus, the efficiency of the simulation procedure strongly depends on the collision kernels B_1 and B_2. The case of the Maxwell pseudo-molecules is significantly simpler than the case of the hard spheres model, and, therefore, we consider the two cases separately. In the algorithms introduced in next subsections, r will always denote different random numbers uniformly distributed on the interval $[0, 1]$.

3.2 Maxwell pseudo-molecules

Here, we choose the constant collision kernels

$$B_1(|\mathbf{v}-\mathbf{w}|, \hat{\omega}) = C_1\,, \quad B_2(|\mathbf{v}-\mathbf{w}|, \hat{\omega}) = C_2\,,$$

and, therefore,

$$E_1(\mathbf{v}_i) = 4\pi\, C_1\, \rho^B\,, \quad E_2(\mathbf{v}_i, \mathbf{v}_j) = 4\pi\, C_2\,, \quad i, j = 1, \ldots, n\,.$$

Thus, we obtain the following efficient simulation algorithm on the time interval $[0, t_{max}]$.

Algorithm 1

1. initialization

   1.1 set time to zero $t = 0$

   1.2 for $i = 1, \ldots, n$
   generate the velocities $\mathbf{v}_i$ according to $f_0(\mathbf{v})$

   1.3 compute the time counter parameters

$$\hat{\pi}_1 = 4\pi\, C_1\, \rho^B\, n\,, \quad \hat{\pi}_2 = 4\pi\, C_2\, \frac{n-1}{2}\,, \quad \hat{\pi} = \hat{\pi}_1 + \hat{\pi}_2$$

2. repeat

   2.1 compute the time counter

$$\tau = -\hat{\pi}^{-1}\ln(r)$$

   2.2 update the time of the system

$$t := t + \tau$$

   stop, if the final time is exceeded, i.e. if $t \geq t_{max}$

2.3 If

$$r \le \frac{\hat{\pi}_1}{\hat{\pi}}$$

perform an elastic collision

2.3.1 define the index i

$$i = [r \cdot n] + 1$$

2.3.2 generate $\mathbf{w}$ according to the density

$$\frac{1}{\rho^B} f^B(\mathbf{w})$$

2.3.3 generate $\hat{\omega} \in S^2$ uniformly

2.3.4 compute the post-collisional velocity

$$\mathbf{v}_i := (1-\alpha)\mathbf{v}_i + \alpha\mathbf{w} + \alpha|\mathbf{v}_i - \mathbf{w}|\,\hat{\omega}$$

2.4 else perform an inelastic binary collision

2.4.1 define the index i

$$i = [r \cdot n] + 1$$

2.4.2 define the index j repeating

$$j = [r \cdot n] + 1$$

until $j \neq i$

2.4.3 generate $\hat{\omega} \in S^2$ uniformly

2.4.4 compute the post-collisional velocities

$$\begin{aligned}
\mathbf{v}_i &:= \frac{1+\beta}{2}\,\mathbf{v}_i + \frac{1-\beta}{2}\,\mathbf{v}_j + \frac{1-\beta}{2}\,|\mathbf{v}_i - \mathbf{v}_j|\,\hat{\omega} \\
\mathbf{v}_j &:= \frac{1-\beta}{2}\,\mathbf{v}_i + \frac{1+\beta}{2}\,\mathbf{v}_j - \frac{1-\beta}{2}\,|\mathbf{v}_i - \mathbf{v}_j|\,\hat{\omega}
\end{aligned}$$

3.3 Hard spheres model

For hard spheres model, we have

$$B_1(|\mathbf{v}-\mathbf{w}|,\hat{\omega}) = C_1|\mathbf{v}-\mathbf{w}|\,, \quad B_2(|\mathbf{v}-\mathbf{w}|,\hat{\omega}) = C_2|\mathbf{v}-\mathbf{w}|\,,$$

and, therefore,

$$\begin{aligned}
E_1(\mathbf{v}_i) &= 4\pi\, C_1 \int\limits_{\mathbb{R}^3} |\mathbf{v}_i - \mathbf{w}| f^B(\mathbf{w})\, d\mathbf{w}\,, \quad i = 1,\dots,n\,, \\
E_2(\mathbf{v}_i,\mathbf{v}_j) &= 4\pi\, C_2 |\mathbf{v}_i - \mathbf{w}_j|, \quad i,j = 1,\dots,n\,.
\end{aligned}$$

The integral in the formula for E_1 can be computed analytically leading to the rather complicated expression

$$E_1(\mathbf{v}_i) = 4\pi\, C_1\, \rho^B \left(\pi^{-1/2}\, b\, \exp\Big(-\frac{a_i^2}{b^2}\Big) + \frac{1}{2}\,(2a_i^2 + b^2)\,\frac{1}{a_i}\,\mathrm{erf}\Big(\frac{a_i}{b}\Big)\right),$$

where

$$a_i = |\mathbf{v}_i - \mathbf{u}^B|\,, \quad b = \left(\frac{2T^B}{m^B}\right)^{1/2}\,, \tag{28}$$

and erf denotes the error function [1]. In the special case $\mathbf{v}_i = \mathbf{u}^B$, i.e. $a = 0$, this expression simplifies to

$$E_1(\mathbf{u}^B) = 8\pi^{1/2}\, C_1\, \rho^B\, b\,.$$

Thus, the direct simulation will require the choice of the collision partners corresponding to unequal discrete probabilities. Furthermore, given i, the velocity $\mathbf{w}$ of the collision partner from the background has to be generated according to the rather complicated density

$$\frac{|\mathbf{v}_i - \mathbf{w}| f^B(\mathbf{w})}{\displaystyle\int_{\mathbb{R}^3} |\mathbf{v}_i - \mathbf{w}| f^B(\mathbf{w})\, d\mathbf{w}}\,.$$

The standard technique to solve this problem, is the introduction of some majorants for the collision frequencies based on the fact that in every simulation the number of particles is finite, and the same occurs to the maximal relative speed between the particles $\mathbf{v}_i$ and the background bulk velocity $\mathbf{u}^B$ in the case of elastic collisions. For the inelastic collisions, we use the similar fact that for a finite particle system the relative speed $|\mathbf{v}_i - \mathbf{v}_j|$ is bounded. Those majorants may depend on time. Thus, for the elastic collisions, we obtain with the majorant

$$\begin{aligned} B_1(|\mathbf{v}-\mathbf{w}|, \hat{\omega}) &= C_1\,|\mathbf{v}-\mathbf{w}| \\ &\le C_1\left(|\mathbf{v}-\mathbf{u}^B| + |\mathbf{w}-\mathbf{u}^B|\right) = B_{1,max}(|\mathbf{v}-\mathbf{w}|, \hat{\omega}) \end{aligned}$$

the following estimate

$$E_1(\mathbf{v}_i) \le E_{1,max}(\mathbf{v}_i) = C_1\,\rho^B\left(4\pi\, a_i + 8\pi^{1/2} b\right)\,,$$

where the notation (28) for the quantities a_i and b has been used. The values $E_{1,max}(\mathbf{v}_i)$ will be now used for the computation of the time counter $\hat{\pi}_1$

$$\hat{\pi}_1 = \sum_{i=1}^{n} E_{1,max}(\mathbf{v}_i)\,.$$

Thus, the choice of the collision partners is still due to unequal discrete probabilities

$$p_i = \frac{E_{1,max}(\mathbf{v}_i)}{\hat{\pi}_1}\,, \quad i = 1, \ldots, n\,.$$

Note that the time counter $\hat{\pi}_1$ is a function of time and it has to be updated after every elastic collision as

$$\hat{\pi}_1(t+\tau) = \hat{\pi}_1(t) - E_{1,max}(\mathbf{v}_i) + E_{1,max}(\mathbf{v}_i')\,,$$

and after every inelastic binary collision as

$$\hat{\pi}_1(t+\tau) = \hat{\pi}_1(t) - E_{1,max}(\mathbf{v}_i) - E_{1,max}(\mathbf{v}_j) + E_{1,max}(\mathbf{v}_i^*) + E_{1,max}(\mathbf{v}_j^*)\,.$$

However, there is significant simplification for the generation of the background particles. The probability density is now

$$p(\mathbf{w}) = \frac{\Big(|\mathbf{v}_i - \mathbf{u}^B| + |\mathbf{w} - \mathbf{u}^B|\Big) f^B(\mathbf{w})}{\displaystyle\int_{\mathbb{R}^3} \Big(|\mathbf{v}_i - \mathbf{u}^B| + |\mathbf{w} - \mathbf{u}^B|\Big) f^B(\mathbf{w})\, d\mathbf{w}}\,.$$

The generating of particles corresponding to this density is as follows. First, we get

$$\int_{\mathbb{R}^3} \Big(|\mathbf{v}_i - \mathbf{u}^B| + |\mathbf{w} - \mathbf{u}^B|\Big) f^B(\mathbf{w})\, d\mathbf{w} = \rho^B(a_i + 2\pi^{-1/2}\, b)\,,$$

where the notations (28) have been used. The density p can be written as a sum

$$p(\mathbf{w}) = \frac{a_i}{a_i + 2\pi^{-1/2}\, b}\, p_1(\mathbf{w}) + \frac{2\pi^{-1/2}\, b}{a_i + 2\pi^{-1/2}\, b}\, p_2(\mathbf{w})\,,$$

where

$$p_1(\mathbf{w}) = \frac{1}{\rho^B} f^B(\mathbf{w})$$

is the normalized background Maxwell distribution and

$$p_2(\mathbf{w}) = \frac{\pi^{1/2}}{2\, b\rho^B}\, |\mathbf{w} - \mathbf{u}^B|\, f^B(\mathbf{w})\,. \tag{29}$$

Thus, with the probability

$$\frac{a_i}{a_i + 2\pi^{-1/2}\, b}$$

the particle will be generated according to the background Maxwell distribution and with the probability

$$\frac{2\pi^{-1/2}\, b}{a_i + 2\pi^{-1/2}\, b}$$

according to the density (29). As the price for this simplification, we have to introduce fictitious collisions, i.e. once the particle i is chosen, the velocity $\mathbf{w}$ of the collision partner from the background is generated, the direction $\hat{\omega}$ (which is uniformly distributed on the unit sphere for the hard spheres model) is sampled, then the collision will be rejected with the probability

$$1 - \frac{B_1(|\mathbf{v}_i - \mathbf{w}|, \hat{\omega})}{B_{1,max}(|\mathbf{v}_i - \mathbf{w}|, \hat{\omega})} = 1 - \frac{|\mathbf{v}_i - \mathbf{w}|}{|\mathbf{v}_i - \mathbf{u}^B| + |\mathbf{w} - \mathbf{u}^B|}\,.$$

Note that due to elastic collisions, which do not conserve the momentum, the bulk velocity

$$\mathbf{u}_n = \frac{1}{n}\sum_{i=1}^{n} \mathbf{v}_i$$

is a function of time, and, therefore, it has to be updated after every elastic collision. Thus, the bulk velocity is not convenient to obtain the majorant for the binary collisions. We will use the constant background bulk velocity $\mathbf{u}^B$ instead and obtain

$$\begin{aligned} E_2(\mathbf{v}_i, \mathbf{v}_j) &= 4\pi\, C_2 |\mathbf{v}_i - \mathbf{v}_j| \le 4\pi\, C_2 \max_{1\le i\ne j\le n} |\mathbf{v}_i - \mathbf{v}_j| \\ &\le 8\pi\, C_2 \max_{1\le i\le n} |\mathbf{v}_i - \mathbf{u}^B| = E_{2,max}\,. \end{aligned}$$

Note that the quantity

$$U_{2,max} = \max_{1\le i\le n} |\mathbf{v}_i - \mathbf{u}^B|$$

has to be updated after every collision as

$$U_{2,max}(t+\tau) = \max\left\{U_{2,max}(t)\,, |\mathbf{v}_i' - \mathbf{u}^B|\right\}$$

after an elastic collision and as

$$U_{2,max}(t+\tau) = \max\left\{U_{2,max}(t)\,, |\mathbf{v}_i^* - \mathbf{u}^B|\,, |\mathbf{v}_j^* - \mathbf{u}^B|\right\}$$

after an inelastic binary collision. At this point, we are finally able to formulate a direct simulation algorithm also for the hard spheres model.

Algorithm 2

1. initialization

   1.1 set time to zero $t = 0$

   1.2 for $i = 1, \ldots, n$
   generate the velocities $\mathbf{v}_i$ according to $f_0(\mathbf{v})$

   1.3 compute the initial majorants

$$E_{1,max}(\mathbf{v}_i) = C_1\, \rho^B \left(4\pi\, a_i + 8\pi^{1/2} b\right)\,, \quad i = 1, \ldots, n\,,$$

   with

$$a_i = |\mathbf{v}_i - \mathbf{u}^B|\,, \quad b = \left(\frac{2T^B}{m^B}\right)^{1/2}$$

   and

$$U_{2,max} = \max_{1\le i\le n} a_i$$

   1.4 compute the initial time counter parameters

$$\hat{\pi}_1 = \sum_{i=1}^{n} E_{1,max}(\mathbf{v}_i)\,, \quad \hat{\pi}_2 = 8\pi\, C_2\, U_{2,max} \frac{n-1}{2}$$

2. repeat

2.1 compute the time counter parameter

$$\hat{\pi} = \hat{\pi}_1 + \hat{\pi}_2$$

2.2 compute the time counter

$$\tau = -\hat{\pi}^{-1} \ln(r)$$

2.3 update the time of the system

$$t := t + \tau$$

stop, if the final time is exceeded, i.e. if $t \geq t_{max}$

2.4 If

$$r \leq \frac{\hat{\pi}_1}{\hat{\pi}}$$

perform an elastic collision

2.4.1 define the index i according to the probabilities

$$p_i = \frac{E_{1,max}(\mathbf{v}_i)}{\hat{\pi}_1}, \quad i = 1, \ldots, n$$

2.4.2 generate $\mathbf{w}$ according to the density

$$\frac{\Big(|\mathbf{v}_i - \mathbf{u}^B| + |\mathbf{w} - \mathbf{u}^B|\Big) f^B(\mathbf{w})}{\displaystyle\int_{\mathbb{R}^3} \Big(|\mathbf{v}_i - \mathbf{u}^B| + |\mathbf{w} - \mathbf{u}^B|\Big) f^B(\mathbf{w})\, d\mathbf{w}}$$

2.4.3 generate $\hat{\omega} \in S^2$ uniformly

2.4.4 if

$$r > \frac{|\mathbf{v}_i - \mathbf{w}|}{|\mathbf{v}_i - \mathbf{u}^B| + |\mathbf{w} - \mathbf{u}^B|}$$

reject the collision and go to Step 2.2

2.4.5 compute the post-collisional velocity

$$\mathbf{v}_i' := (1 - \alpha)\mathbf{v}_i + \alpha \mathbf{w} + \alpha |\mathbf{v}_i - \mathbf{w}|\, \hat{\omega}$$

2.4.6 update the time counter parameters

$$\begin{aligned}
\hat{\pi}_1 &:= \hat{\pi}_1 - E_{1,max}(\mathbf{v}_i) + E_{1,max}(\mathbf{v}_i') \\
E_{1,max}(\mathbf{v}_i) &:= E_{1,max}(\mathbf{v}_i') \\
U_{2,max} &:= \max\left\{U_{2,max}\,, |\mathbf{v}_i' - \mathbf{u}^B|\right\} \\
\hat{\pi}_2 &:= 8\pi\, C_2\, U_{2,max} \frac{n-1}{2}
\end{aligned}$$

2.4.7 replace the velocity

$$\mathbf{v}_i := \mathbf{v}_i'$$

2.5 else perform an inelastic binary collision

2.5.1 define the index i

$$i = [r \cdot n] + 1$$

2.5.2 define the index j repeating

$$j = [r \cdot n] + 1$$

until $j \neq i$

2.5.3 generate $\hat{\omega} \in S^2$ uniformly

2.5.4 if

$$r > \frac{|\mathbf{v}_i - \mathbf{v}_j|}{2\, U_{2,max}}$$

reject the collision and go to Step 2.2

2.5.5 compute the post-collisional velocities

$$\begin{aligned} \mathbf{v}_i^* &:= \frac{1+\beta}{2}\,\mathbf{v}_i + \frac{1-\beta}{2}\,\mathbf{v}_j + \frac{1-\beta}{2}\,|\mathbf{v}_i - \mathbf{v}_j|\,\hat{\omega} \\ \mathbf{v}_j^* &:= \frac{1-\beta}{2}\,\mathbf{v}_i + \frac{1+\beta}{2}\,\mathbf{v}_j - \frac{1-\beta}{2}\,|\mathbf{v}_i - \mathbf{v}_j|\,\hat{\omega} \end{aligned}$$

2.5.6 update the time counter parameters

$$\begin{aligned} \hat{\pi}_1 &:= \hat{\pi}_1 - E_{1,max}(\mathbf{v}_i) - E_{1,max}(\mathbf{v}_j) \\ &\quad + E_{1,max}(\mathbf{v}_i^*) + E_{1,max}(\mathbf{v}_j^*) \\ E_{1,max}(\mathbf{v}_i) &:= E_{1,max}(\mathbf{v}_i^*)\,, \quad E_{1,max}(\mathbf{v}_j) := E_{1,max}(\mathbf{v}_j^*) \\ U_{2,max} &:= \max\left\{U_{2,max}\,, |\mathbf{v}_i^* - \mathbf{u}^B|\,, |\mathbf{v}_j^* - \mathbf{u}^B|\right\} \\ \hat{\pi}_2 &:= 8\pi\, C_2\, U_{2,max}\frac{n-1}{2} \end{aligned}$$

2.5.7 replace the velocities

$$\mathbf{v}_i := \mathbf{v}_i^*\,, \quad \mathbf{v}_j := \mathbf{v}_j^*$$

Note that the procedure to choose the particle index i for the elastic collision with the background in step 2.4.1 is realized by the use of the alias algorithm first introduced by Walker in 1974, see [31] for more details. The alias algorithm requires only $\mathcal{O}(1)$ arithmetical operations for a sample instead of $\mathcal{O}(n)$ when the standard algorithm, choosing i so that

$$\sum_{j=1}^{i-1} p_j < r \leq \sum_{j=1}^{i} p_j\,,$$

where r denotes a random number uniformly distributed on $(0, 1)$, is used.

4 Numerical Examples

4.1 Statistical notions

In this subsection, we introduce some definitions and notations that are helpful for the understanding of stochastic numerical procedures. Functionals of the form (cf. (8))

$$F(t) = \int_{\mathbb{R}^3} \varphi(\mathbf{v})\, f(t, \mathbf{v})\, d\mathbf{v} \tag{30}$$

are approximated by the random variable

$$\xi^{(n)}(t) = \frac{1}{n} \sum_{i=1}^{n} \varphi(\mathbf{v}_i(t))\,, \tag{31}$$

here $\mathbf{v}_1(t), \ldots, \mathbf{v}_n(t)$ are the velocities of the particles. In order to estimate and to reduce the random fluctuations of the estimator (31), a number N of independent ensembles of particles is generated. The corresponding values of the random variable are denoted by

$$\xi_1^{(n)}(t), \ldots, \xi_N^{(n)}(t)\,.$$

The empirical mean value of the random variable (31)

$$\eta_1^{(n,N)}(t) = \frac{1}{N} \sum_{j=1}^{N} \xi_j^{(n)}(t) \tag{32}$$

is then used as an approximation to the functional (30). The error of this approximation is

$$e^{(n,N)}(t) = |\eta_1^{(n,N)}(t) - F(t)|$$

and consists of the following two components. The systematic error is the difference between the mathematical expectation of the random variable (31) and the exact value of the functional, i.e.

$$e_{sys}^{(n)}(t) = E\xi^{(n)}(t) - F(t)\,.$$

The statistical error is the difference between the empirical mean value and the expected value of the random variable, i.e.

$$e_{stat}^{(n,N)}(t) = \eta_1^{(n,N)}(t) - E\xi^{(n)}(t)\,.$$

A confidence interval for the expectation of the random variable $\xi^{(n)}(t)$ is obtained as

$$I_p = \left[\eta_1^{(n,N)}(t) - \lambda_p \sqrt{\frac{\operatorname{Var} \xi^{(n)}(t)}{N}}\,,\ \eta_1^{(n,N)}(t) + \lambda_p \sqrt{\frac{\operatorname{Var} \xi^{(n)}(t)}{N}} \right], \tag{33}$$

where

$$\operatorname{Var}\xi^{(n)}(t) = E\left[\xi^{(n)}(t) - E\xi^{(n)}(t)\right]^2 = E\left[\xi^{(n)}(t)\right]^2 - \left[E\xi^{(n)}(t)\right]^2 \tag{34}$$

is the variance of the random variable (31), and $p \in (0,1)$ is the confidence level. This means that

$$\operatorname{Prob}\Big\{E\xi^{(n)}(t) \notin I_p\Big\} = \operatorname{Prob}\left\{|e_{stat}^{(n,N)}(t)| \geq \lambda_p\sqrt{\frac{\operatorname{Var}\xi^{(n)}(t)}{N}}\right\} \sim p\,.$$

Thus, the value

$$c^{(n,N)}(t) = \lambda_p\sqrt{\frac{\operatorname{Var}\xi^{(n)}(t)}{N}}$$

is a probabilistic upper bound for the statistical error. In the calculations, we use a confidence level of $p = 0.999$ and $\lambda_p = 3.2$. The variance is approximated by the corresponding empirical value (cf. (34)), i.e.

$$\operatorname{Var}\xi^{(n)}(t) \sim \eta_2^{(n,N)}(t) - \left[\eta_1^{(n,N)}(t)\right]^2,$$

where

$$\eta_2^{(n,N)}(t) = \frac{1}{N}\sum_{j=1}^{N}\left[\xi_j^{(n)}(t)\right]^2$$

is the empirical second moment of the random variable (31).

4.2 Maxwell pseudo-molecules

We use the following distribution

$$f_0(\mathbf{v}) = \alpha_{ini} f_{M_1}(\mathbf{v}) + (1-\alpha_{ini}) f_{M_2}(\mathbf{v})\,, \tag{35}$$

where f_M denotes the Maxwell distribution

$$f_M(\mathbf{v}) = \left(\frac{m}{2\pi T}\right)^{3/2}\exp\left(-\frac{m}{2T}|\mathbf{v}-\mathbf{u}|^2\right), \tag{36}$$

as the initial condition.

Example 1 *The following set of parameters has been used in (35):*

$$\alpha_{ini} = 1/2$$

and

$$\begin{aligned} m_1 &= 1\,,\ \mathbf{u}_1 = (-2,2,0)^\top,\ T_1 = 1\,,\\ m_2 &= 1\,,\ \mathbf{u}_2 = (+2,0,0)^\top,\ T_2 = 1\,. \end{aligned}$$

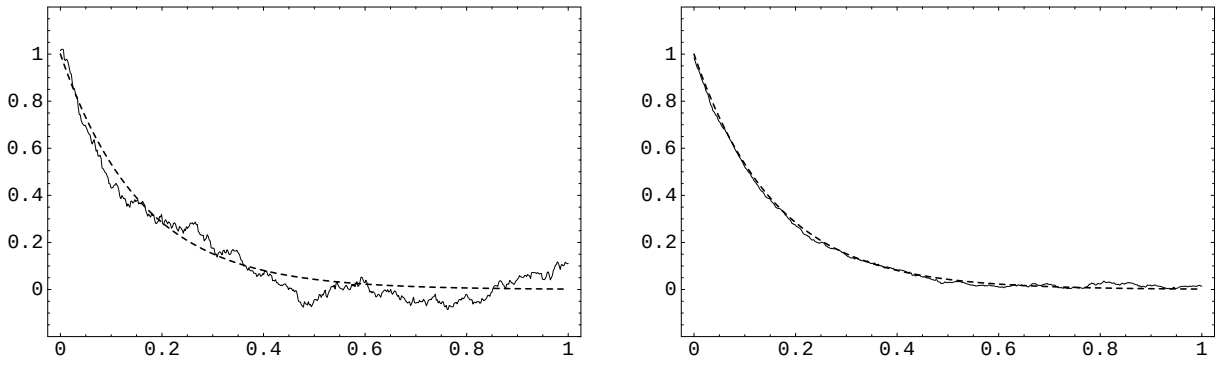

Figure 1: Time relaxation of the bulk velocity, Example 1, $n = 4, 16$

Thus, we obtain that the initial number density (which remains conserved) is equal to one and

$$\mathbf{u}_0 = (0, 1, 0)^\top \,, \; T_0 = 8/3 \,.$$

The parameters of the background Maxwell distribution are

$$\rho^B = 1 \,, \; m^B = 1 \,, \; \mathbf{u}^B = (0, 0, 0)^\top \,, \; T^B = 1 \,.$$

The collision kernels of both collision operators J_{EL} and J_{IN} are assumed to be constant

$$B_1(|\mathbf{v} - \mathbf{w}|, \hat{\omega}) = C_1 = B_2(|\mathbf{v} - \mathbf{w}|, \hat{\omega}) = C_2 = 1 \,.$$

Finally, we choose the restitution coefficient $e = 1/2$.

Thus, we get $\alpha = 1/2$, $Kn = 1$, and the exact relaxation of the bulk velocity is (cf. (14))

$$\mathbf{u}(t) = \begin{pmatrix} 0 \\ 1 \\ 0 \end{pmatrix} \exp\Big(- 2\pi \, t \Big) \,. \tag{37}$$

The exact relaxation of the temperature is (cf. (15))

$$\begin{aligned} T(t) \;\; &= \;\; \frac{8}{3} \exp\Big(- \frac{11}{4} \pi \, t \Big) + \frac{8}{11} \Big(1 - \exp\Big(- \frac{11}{4} \pi \, t \Big) \Big) \\ &- \;\; \frac{8}{15} \Big(\exp\Big(- 4\pi \, t \Big) - \exp\Big(- \frac{11}{4} \pi \, t \Big) \Big) \,, \end{aligned} \tag{38}$$

and the asymptotic equilibrium value is $T^* = 8/11$. In Figure 1, the thick dashed line represents the course of the second component u_2 of the analytical solution (37) on the time interval $[0, 1]$ while the thin line shows the course of the empirical mean value (32) for this quantity. The left plot corresponds to $n = 4$ particles by averaging of $N_{rep} = 64$ independent ensembles while the right plot is due to $n = 16$ and $N_{rep} = 256$. An excellent agreement between analytical and numerical results can be seen. For higher values of n and N_{rep} the corresponding curves can not be optically distinguished. In Figure 2, the

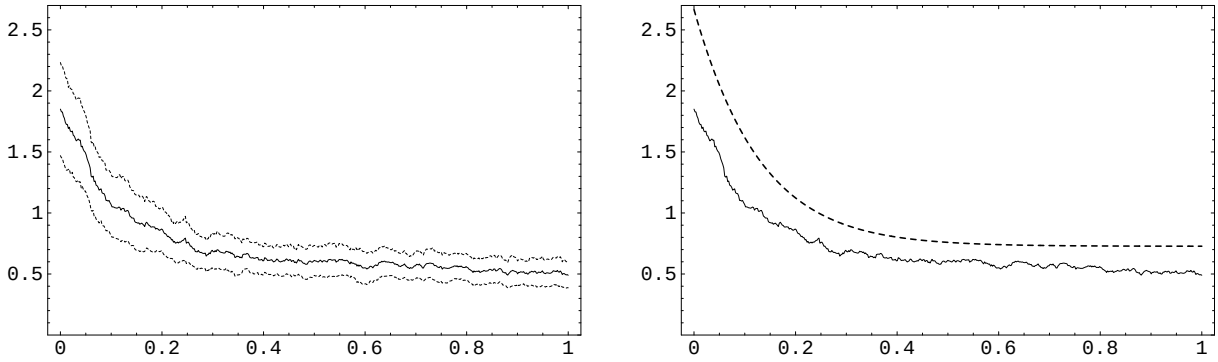

Figure 2: Time relaxation of the temperature, Example 1, $n = 4$

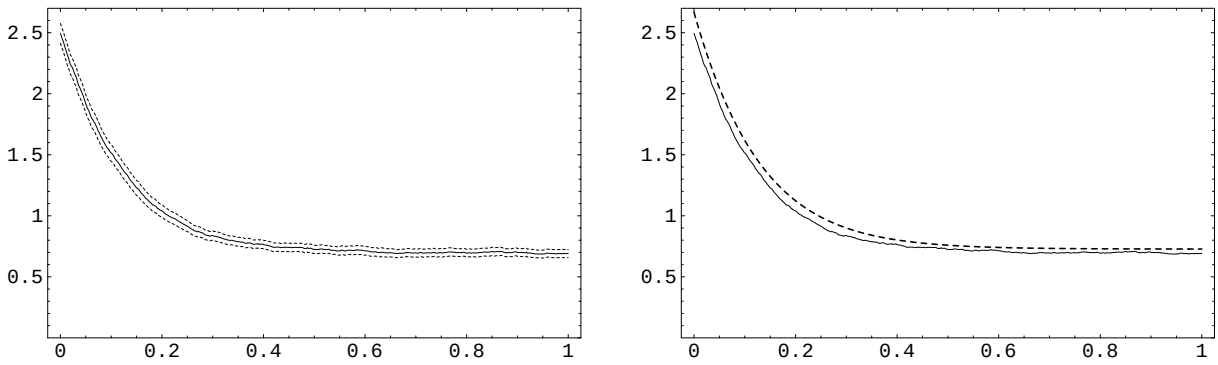

Figure 3: Time relaxation of the temperature, Example 1, $n = 16$

Table 1: Convergence of the temperature, Example 1

n	N_{rep}	Err	CF	$Conf$	CF
4	64	$3.49 \cdot 10^{-1}$	-	$1.15 \cdot 10^{+0}$	-
16	256	$8.80 \cdot 10^{-2}$	3.97	$2.50 \cdot 10^{-1}$	4.60
64	1024	$1.99 \cdot 10^{-2}$	4.42	$6.41 \cdot 10^{-2}$	3.90
256	4096	$5.51 \cdot 10^{-3}$	3.61	$1.62 \cdot 10^{-2}$	3.96
1024	16384	$1.08 \cdot 10^{-3}$	5.10	$3.99 \cdot 10^{-3}$	4.06

exact course of the temperature (38) is again represented by the thick dashed line on the right plot while the thin solid line shows its empirical mean value on both plots. The pair of thin dashed lines on the left plot represents the confidence intervals (33) obtained for $n = 4$ by averaging of $N_{rep} = 64$ independent ensembles. In Figure 3, the same objects are plotted for $n = 16$ and $N_{rep} = 1024$. In Table 1, the convergence history for the temperature is presented. The number of particles is listed in the first column of this table. The second column contains the number of independent ensembles generated, while the third column of Table 1 shows the relative error for the temperature, i.e. the maximal relative deviation of the exact values for the temperature from its empirical mean value (32) considered in 513 uniform time points on the time interval $[0, 1]$

$$Err = \max_{0 \le i \le 512} \left| \frac{T(t_i) - \eta_1^{(n,N_{rep})}(t_i)}{T(t_i)} \right| , \quad t_i = \frac{1}{512}\, i \,,\ i = 0, \ldots, 512 \,.$$

The fourth column of this table shows rate of convergence, i.e. the quotient between the errors in two consecutive lines of column three. The thickness of the confidence bands (33) is listed in the next column while the last column shows the rate of convergence of this quantity. From theoretical point of view, we expect a linear convergence of the error, i.e. $Err = \mathcal{O}(1/n)$ and $Conf = \mathcal{O}(1/\sqrt{n\, N_{rep}})$. Both asymptotics can be cleanly seen in Table 1. Thus, Algorithm 1 presented in Section 3 behaves according to the theory. In Figure 4, the histograms (thick, dashed lines) of the integrated distribution function

$$f_1(t, v_1) = \int\limits_{\mathbb{R}^2} f(t, \mathbf{v})\, dv_2 dv_3$$

are shown. The left plot corresponds to the initial distribution, while the "final" distribution is shown in the right plot. The thin lines show the Maxwell distribution with the parameters of the distribution f. Bulk velocity remains constant and one can notice the significant variation of temperature.

Example 2 *Now we start with a Maxwell distribution, i.e. we choose*

$$\alpha_{ini} = 1$$

and

$$m_1 = 1 \,,\ \mathbf{u}_1 = (0, 0, 0)^\top \,,\ T_1 = 1$$

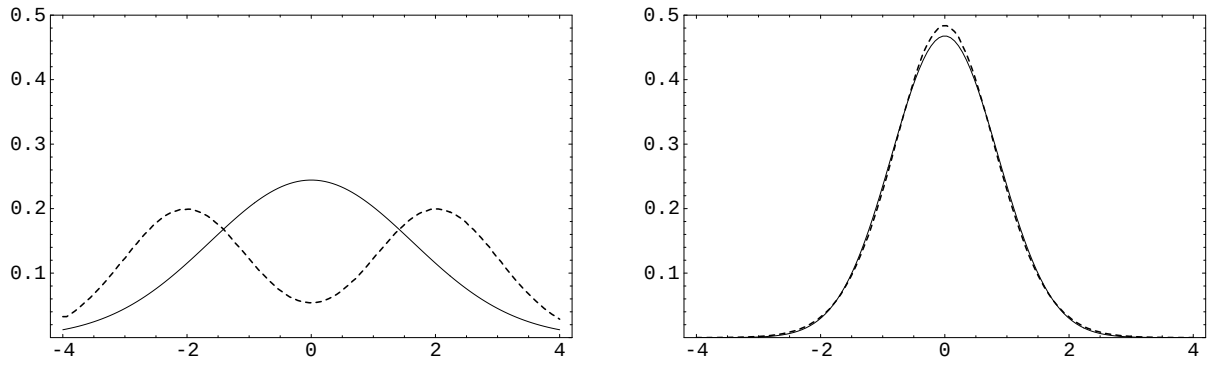

Figure 4: Histograms of the integrated distribution function, Example 1, $n = 1024$

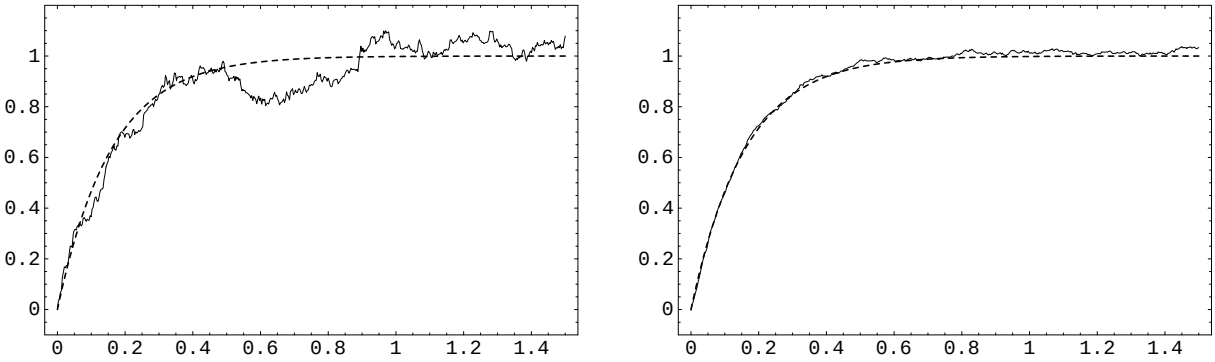

Figure 5: Time relaxation of the bulk velocity, Example 2, $n = 4, 16$

Thus, we obtain

$$\mathbf{u}_0 = (0,0,0)^\top\,,\ T_0 = 1\,.$$

The parameters of the background Maxwell distribution are

$$\rho^B = 1\,,\ m^B = 1\,,\ \mathbf{u}^B = (0,1,0)^\top\,,\ T^B = 1\,.$$

The collision kernels of the both collision operators J_{EL} and J_{IN} are assumed to be constant

$$B_1(|\mathbf{v}-\mathbf{w}|,\hat{\omega}) = C_1 = 1\,,\quad B_2(|\mathbf{v}-\mathbf{w}|,\hat{\omega}) = C_2 = 1/8\,.$$

i.e. we consider a rather weak inelastic binary collision operator ($Kn = 1/8$).

In Figure 5, the results of the computations for $n = 4$ and $N_{rep} = 64$ as well as for $n = 16$ and $N_{rep} = 256$ are presented. Again, an excellent agreement between analytical and numerical results can be seen even for very small values of the parameter n. The exact relaxation of the bulk velocity is now

$$\mathbf{u}(t) = \begin{pmatrix} 0 \\ 1 \\ 0 \end{pmatrix} \Big(1 - \exp\Big(-2\pi\, t\Big)\Big)\,.$$

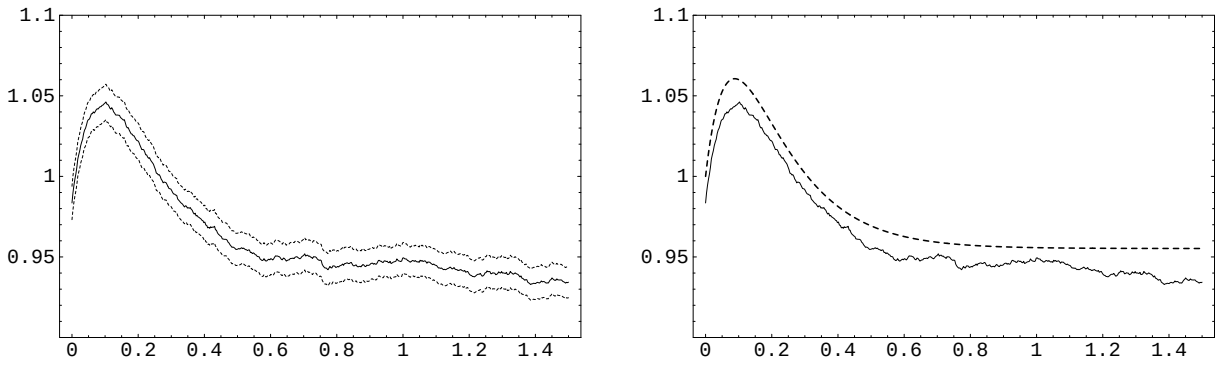

Figure 6: Time relaxation of the temperature, Example 2, $n = 64$

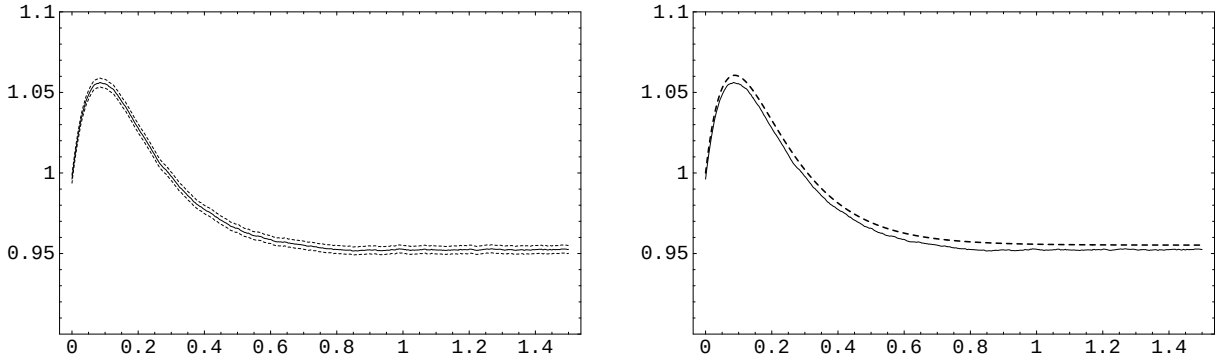

Figure 7: Time relaxation of the temperature, Example 2, $n = 256$

The corresponding temperature is

$$\begin{aligned} T(t) &= \exp\Big(-\frac{67}{32}\pi\, t\Big) + \frac{64}{67}\Big(1 - \exp\Big(-\frac{67}{32}\pi\, t\Big)\Big) \\ &- \frac{64}{183}\Big(\exp\Big(-4\pi\, t\Big) - \exp\Big(-\frac{67}{32}\pi\, t\Big)\Big) \end{aligned}$$

with $T^* = 64/67$, and exhibits an overshoot at the beginning of the relaxation. In Figure 6, the numerical results are presented for $n = 64$ by averaging of $N_{rep} = 1024$ independent ensembles. In Figure 7, the same objects are plotted for $n = 256$ and $N_{rep} = 4096$. In Table 2, the convergence history for the temperature is presented. Thus, Algorithm 1 behaves again according to the theory. In Figure 8, the histograms of the

Table 2: Convergence of the temperature, Example 2

n	N_{rep}	Err	CF	$Conf$	CF
4	64	$3.14 \cdot 10^{-1}$	-	$1.99 \cdot 10^{-1}$	-
16	256	$9.20 \cdot 10^{-2}$	3.41	$4.51 \cdot 10^{-2}$	3.68
64	1024	$2.34 \cdot 10^{-2}$	3.93	$1.13 \cdot 10^{-2}$	3.99
256	4096	$5.71 \cdot 10^{-3}$	4.10	$2.73 \cdot 10^{-3}$	4.14
1024	16384	$1.48 \cdot 10^{-3}$	3.86	$6.80 \cdot 10^{-4}$	4.01

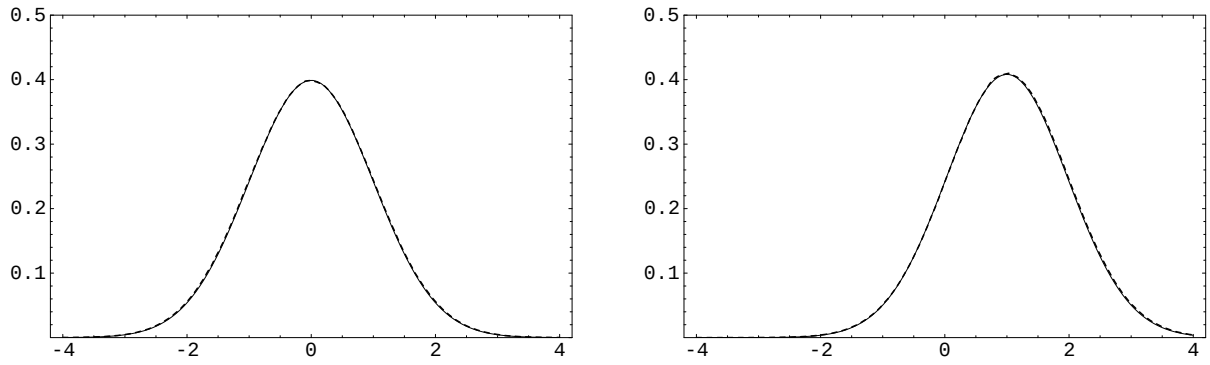

Figure 8: Histograms of the integrated distribution function, Example 2, $n = 1024$

second component of the solution (thick, dashed lines) at the begin and at the end of the relaxation are shown together with the corresponding Maxwell distributions (thin lines). Now the slight decrease of temperature is accompanied by a shift of drift velocity from zero to one.

Example 3 *We use the same parameters as in Example 2 except the mass of the background particles which is now more realistic*

$$m^B = 1/8\,.$$

The exact relaxation of the bulk velocity is now

$$\mathbf{u}(t) = \begin{pmatrix} 0 \\ 1 \\ 0 \end{pmatrix} \Big(1 - \exp\Big(-4/9\pi\, t\Big)\Big)\,.$$

The corresponding temperature is

$$\begin{aligned} T(t) &= \exp\Big(-\frac{2291}{2592}\pi\, t\Big) + \frac{2048}{2291}\Big(1 - \exp\Big(-\frac{2291}{2592}\pi\, t\Big)\Big) \\ &- \frac{256}{39}\Big(\exp\Big(-\frac{8}{9}\pi\, t\Big) - \exp\Big(-\frac{2291}{2592}\pi\, t\Big)\Big) \end{aligned}$$

with $T^* = 2048/2291$. The relaxation is slower (exchange of momentum and energy with background is most effective when masses are equal) and the temperature curve does not exhibit an overshoot, see Figures 9, 10.

4.3 Hard spheres model

Example 4 *We consider the set of parameters of Example 2. However, the collision kernels are now*

$$B_1(|\mathbf{v}-\mathbf{w}|, \hat{\omega}) = |\mathbf{v}-\mathbf{w}|\,, \quad B_2(|\mathbf{v}-\mathbf{w}|, \hat{\omega}) = \frac{1}{8}|\mathbf{v}-\mathbf{w}|$$

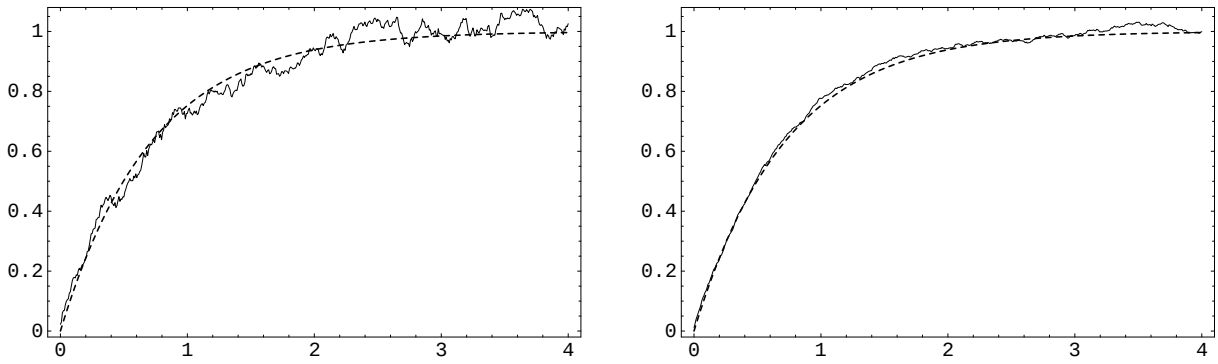

Figure 9: Time relaxation of the bulk velocity, Example 3, $n = 4, 16$

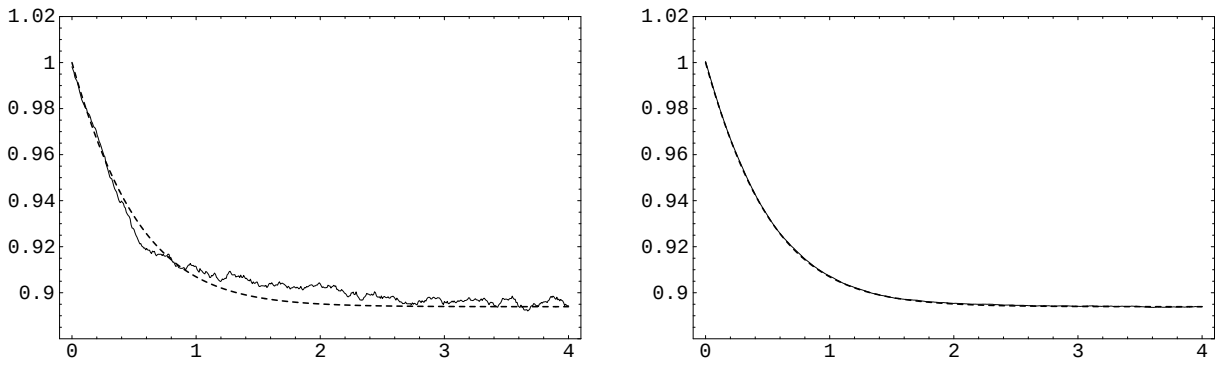

Figure 10: Time relaxation of the temperature, Example 3, $n = 64, 1024$

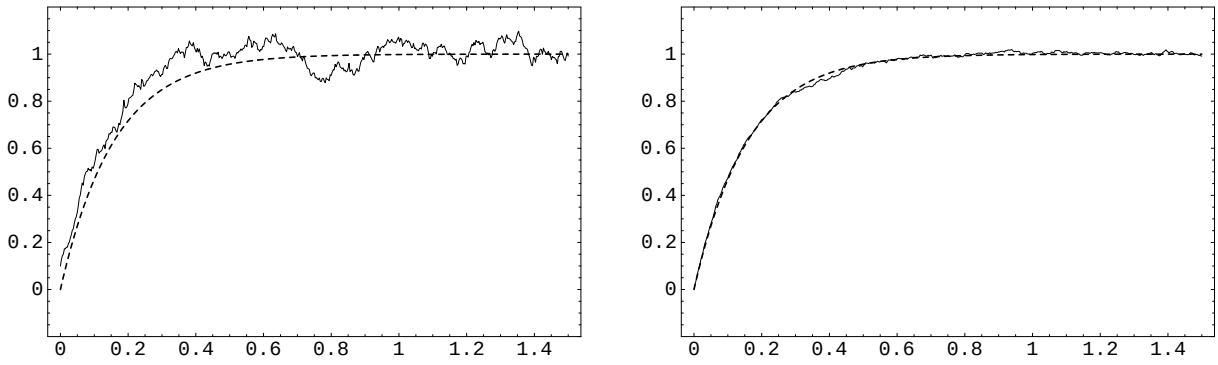

Figure 11: Time relaxation of the bulk velocity, Example 4, $n = 4, 16$

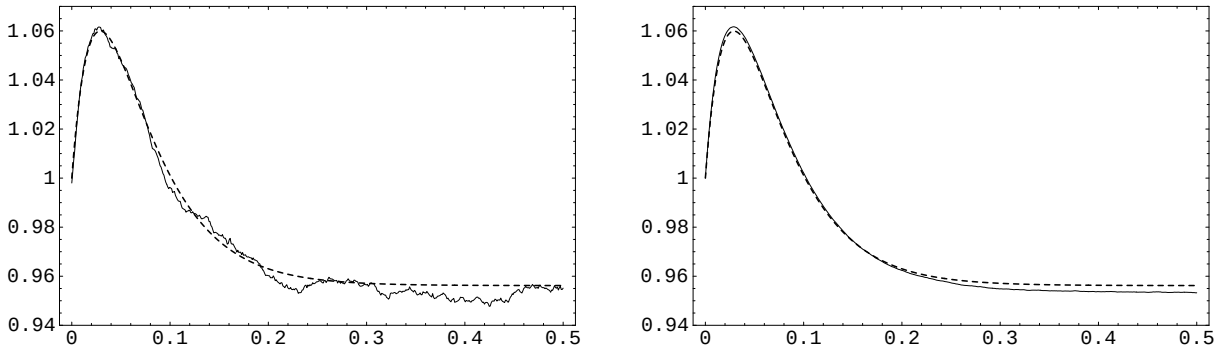

Figure 12: Time relaxation of the temperature, Example 4, $n = 64, 1024$

thus with $\mathcal{K} = Kn = 1/8$. Equilibrium temperature turns out to be $T^* = 0.953$, while the two considered hydrodynamic models yield the same asymptotic value, if rounded off at the third digit, namely $T^* = 0.956$, slightly above the kinetic value. Differences between the two hydrodynamic trends are not visible in the plots. In Figure 11, the thin solid lines show the courses of the numerical solution for the second component of the bulk velocity while the dashed thick lines represent now the numerical solution of the system of ordinary differential equations (22) obtained by the use of the Runge-Kutta scheme of the second order of accuracy. It is remarkable how perfectly both curves coincide already for $n = 16$. In Figure 12, the time relaxation of the temperature for $n = 256$ and $n = 1024$ is shown. On the right plot, where neither the stochastic nor the deterministic errors are visible, the difference between the solution of the Boltzmann equation and of the hydrodynamic model (22) is small but clear. Reliability of the latter model is guaranteed in fact only for $\mathcal{K} \to 0$. Again, we detect an excellent agreement between the models and an high accuracy of Algorithm 2.

Example 5 *In this example, we increase the role of inelastic collisions with the following collision kernels*

$$B_1(|\mathbf{v} - \mathbf{w}|, \hat{\omega}) = |\mathbf{v} - \mathbf{w}|\,, \quad B_2(|\mathbf{v} - \mathbf{w}|, \hat{\omega}) = |\mathbf{v} - \mathbf{w}|\,.$$

Now the parameter $\mathcal{K}$ is unity, thus very far from being small, as required by hydrodynamic equations (21), (22) in order to be reliable. Agreement with the present kinetic

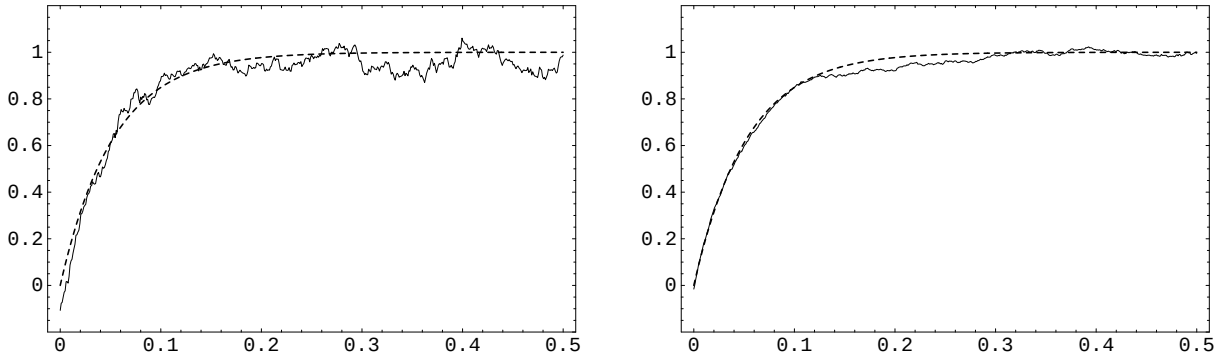

Figure 13: Time relaxation of the bulk velocity, Example 5, $n = 4, 16$

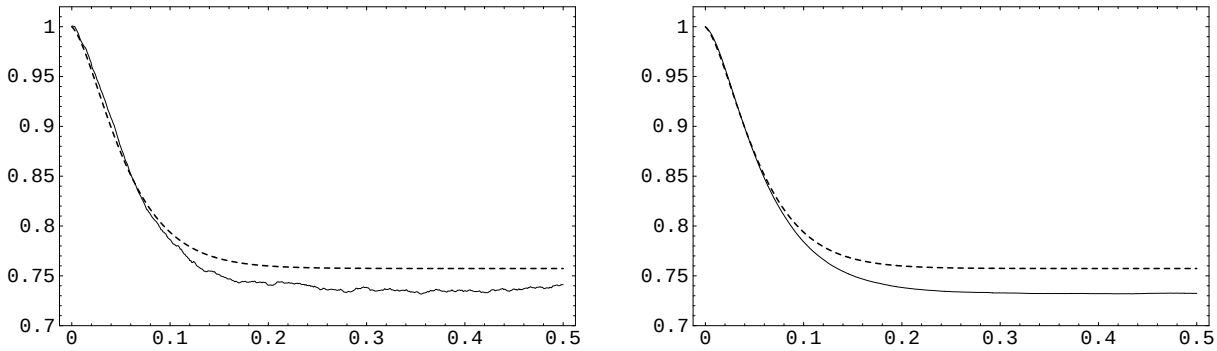

Figure 14: Time relaxation of the temperature, Example 5, $n = 64, 1024$

calculations is then not expected. In Figure 13, the thin solid lines show the courses of the numerical solution for the second component of the bulk velocity while the dashed thick lines represent again the numerical solution of the system of ordinary differential equations (22). In Figure 14, the time relaxation of the temperature for $n = 256$ and $n = 1024$ is shown. The temperature now does not exhibit an overshoot and the difference between the solution of the Boltzmann equation and the hydrodynamic model (22) is much more clear, as it should since we are out of the range of validity of any hydrodynamic limit. Equilibrium temperature from the stochastic simulation turns out to be $T^* = 0.732$, in front of an asymptotic limit from (22) given by $T^* = 0.757$, quite overestimated. One can observe instead the correct evolution predicted by (22) for the bulk velocity, which indeed is not affected by the parameter $\mathcal{K}$. Now the hydrodynamic model (21) does not coincide with (22), and actually, in spite of its unreliability, it would provide a better approximation of the kinetic trend, with an asymptotic equilibrium value $T^* = 0.743$ quite closer to reality. So, the present calculations seem to indicate, as a nice byproduct, that the approximation (21) is more robust than (22) when extended out of the domain of validity of hydrodynamics.

Acknowledgment

Work performed in the frame of activities sponsored by INdAM-GNFM, by the University of Parma (Italy), and by the Universität des Saarlandes (Germany). The first two authors are grateful for the hospitality of the Isaac Newton Institute for Mathematical Sciences, Cambridge, where the present work was completed during the programme "Partial Differential Equations in Kinetic Theories" in September 2010.

References

[1] M. Abramowitz, I.A. Stegun Eds., *Handbook of Mathematical Functions*, Dover, New York (1965).

[2] A. Baldassarri, U. Marini Bettolo Marconi, A. Puglisi, A. Vulpiani, Driven granular gas with gravity, *Phys. Rev. E* **64** (2001), 011301.

[3] D. Benedetto, E. Caglioti, M. Pulvirenti, A kinetic equation for granular media, *Math. Mod. Num. Anal.* **23** (1997), 147–168.

[4] E. Ben Naim, P.L. Krapivski, Multiscaling in inelastic collisions, *Phys. Rev. E* **61** (2000), R5–R8.

[5] T. Biben, P.A. Martin, J. Piasecki, Stationary state of thermostated inelastic hard spheres, *Physica A* **310** (2002), 308–324.

[6] G.A. Bird, *Molecular Gas Dynamics and the Direct Simulation of Gas Flows*, Claredon, Oxford (1994).

[7] M. Bisi, J.A. Carrillo, B. Lods, Equilibrium solution to the inelastic Boltzmann equation driven by a particle bath, *J. Stat. Phys.* **133** (2008), 841–870.

[8] M. Bisi, G. Spiga, Fluid-dynamic equations for granular particles in a host-medium, *J. Math. Phys.* **46** (2005), 113301 (1-20).

[9] M. Bisi, G. Spiga, Dilute granular flows in a medium, *Transp. Theory Stat. Phys.* **36** (2007), 79–105.

[10] M. Bisi, G. Spiga, G. Toscani, Grad's equations and hydrodynamics for weakly inelastic granular flows, *Phys. Fluids* **16** (2004), 4235–4247.

[11] A.V. Bobylev, The theory of the nonlinear spatially uniform Boltzmann equation for Maxwell molecules, *Sov. Sci. Rev. C. Math. Phys.* **7** (1988), 111–233.

[12] A.V. Bobylev, J.A. Carrillo, I. Gamba, On some properties of kinetic and hydrodynamic equations for inelastic interactions, *J. Statist. Phys.* **98** (2000), 743–773; Erratum on: *J. Statist. Phys.* **103**, (2001), 1137–1138.

[13] A.V. Bobylev, C. Cercignani, Self-similar solutions of the Boltzmann equation and their applications, *J. Statist. Phys.* **106** (2002), 1039–1071.

[14] A.V. Bobylev, M. Groppi, G. Spiga, Approximate solutions to the problem of stationary shear flow of smooth granular materials, *Eur. J. Mech. B Fluids* **21** (2002), 91–103.

[15] J.J. Brey, J.W. Dufty, C.S. Kim, A. Santos, Hydrodynamics for granular flows at low density, *Phys. Rev. E* **58** (1998), 4638–4653.

[16] N.V. Brilliantov, T. Pöschel, Granular gases with impact-velocity dependent restitution coefficient. In *Granular Gases*, T. Pöschel, S. Luding Eds. Lecture Notes in Physics, Vol. **564**, Springer Verlag, Berlin (2000), 100–124.

[17] N.V. Brilliantov, T. Pöschel, *Kinetic Theory of Granular Gases*, Oxford University Press, Oxford (2004).

[18] C. Cercignani, *The Boltzmann Equation and its Applications*, Springer, New York (1988).

[19] S. Chapman, T.G. Cowling, *The mathematical theory of non–uniform gases*, Cambridge University Press, Cambridge (1970).

[20] J.J. Duderstadt, W.R. Martin, *Transport Theory*, Wiley (1979).

[21] M.H. Ernst, R. Brito, High energy tails for inelastic Maxwell models, *Europhys. Lett.* **43** (2002), 497–502.

[22] I.M. Gamba, S. Rjasanow, W. Wagner, Direct simulation of the uniformly heated granular Boltzmann equation, *Math. Comput. Modelling* **42** (2005), 683–700.

[23] A. Goldshtein, M. Shapiro, Mechanics of collisional motion of granular materials. Part 1. General hydrodynamic equations, *J. Fluid Mech.* **282** (1995), 75–114.

[24] H. Hayakawa, Hydrodynamics of driven granular gases, *Phys. Rev. E* **68** (2003), 031304.

[25] B. Lods, G. Toscani, The dissipative linear Boltzmann equation for hard spheres, *J. Statist. Phys.* **117** (2004), 635–664.

[26] S. McNamara, W.R. Young, Kinetics of a one–dimensional granular medium in the quasi–elastic limit, *Phys. Fluids A* **5** (1993), 34–45.

[27] J.M. Montanero, V. Garzó, Rheological properties in a low–density granular mixture, *Physica A: Stat. Mech. and Appl.* **310** (2002), 17–38.

[28] S. Rjasanow, W. Wagner, *Stochastic Numerics for the Boltzmann Equation*, number **37** in Springer Series in Computational Mathematics, Springer, Berlin–Heidelberg–New york (2005).

[29] S. Rjasanow, W. Wagner, Time splitting error in DSMC schemes for the spatially homogeneous inelastic Boltzmann equation, *SIAM J. Numer. Anal.* **45** (2007), 54–67.

[30] A. Santos, Granular fluid thermostated by a bath of elastic hard spheres, *Phys. Rev. E* **67** (2003), 051101.

[31] J.C. Smith, S.H. Jacobson, An analysis of the alias method for discrete random–variate generation, *INFORMS Journal on Computing* **17** (2005), 321–327.

[32] G. Spiga, G. Toscani, The dissipative linear Boltzmann equation, *Appl. Math. Lett.* **17** (2004), 295–301.

[33] G. Toscani, Kinetic and hydrodynamic models of nearly elastic granular flows, *Monatsh. Math.* **142** (2004), 179–192.

[34] W. Wagner, Deviational particle Monte Carlo for the Boltzmann equation, *Monte Carlo Methods and Applications* **14** (2008), 191–268.